JOURNAL OF BACTERIOLOGY, June 2009, p. 3772–3784 Vol. 191, No. 12
0021-9193/09/$08.00+0 doi:10.1128/JB.00179-09

ATP-Binding Site Lesions in FtsE Impair Cell Division▽†

S. J. Ryan Arends, Ryan J. Kustusch, and David S. Weiss*

Department of Microbiology, University of Iowa, Iowa City, Iowa 52242

Received 10 February 2009/Accepted 8 April 2009

FtsE and FtsX of *Escherichia coli* constitute an apparent ABC transporter that localizes to the septal ring. In the absence of FtsEX, cells divide poorly and several membrane proteins essential for cell division are largely absent from the septal ring, including FtsK, FtsQ, FtsI, and FtsN. These observations, together with the fact that *ftsE* and *ftsX* are cotranscribed with *ftsY*, which helps to target some proteins for insertion into the cytoplasmic membrane, suggested that FtsEX might contribute to insertion of division proteins into the membrane. Here we show that this hypothesis is probably wrong, because cells depleted of FtsEX had normal amounts of FtsK, FtsQ, FtsI, and FtsN in the membrane fraction. We also show that FtsX localizes to septal rings in cells that lack FtsE, arguing that FtsX targets the FtsEX complex to the ring. Nevertheless, both proteins had to be present to recruit further Fts proteins to the ring. Mutant FtsE proteins with lesions in the ATP-binding site supported septal ring assembly (when produced together with FtsX), but these rings constricted poorly. This finding implies that FtsEX uses ATP to facilitate constriction rather than assembly of the septal ring. Finally, topology analysis revealed that FtsX has only four transmembrane segments, none of which contains a charged amino acid. This structure is not what one would expect of a substrate-specific transmembrane channel, leading us to suggest that FtsEX is not really a transporter even though it probably has to hydrolyze ATP to support cell division.

Cell division in *Escherichia coli* is carried out by ~20 proteins that localize to the midcell, where they form a structure called the septal ring (also called the divisome or septalsome) (4, 27, 55, 57). One component of the septal ring is an apparent ABC transporter composed of the integral membrane protein FtsX and its associated cytoplasmic ATPase, FtsE (15, 47). FtsE and FtsX are widely conserved among gram-negative and gram-positive bacteria. *ftsE* and/or *ftsX* mutants exhibit division defects in *E. coli*, *Neisseria gonorrhoeae*, *Aeromonas hydrophila*, and *Flavobacterium johnsoniae*, indicating that FtsEX function in cell division is conserved in these organisms (33, 40, 43, 45). In contrast, FtsEX of *Bacillus subtilis* has no obvious role in cell division but instead regulates entry into sporulation (24).

One interesting property of *E. coli ftsEX* null mutants is that they can be rescued by a variety of osmotic protectants (44). For example, when grown in LB containing >0.5% NaCl, an *E. coli ftsEX* null mutant is viable and only mildly filamentous, but upon shift to LB lacking NaCl, the cells become filamentous and die (20, 47). A shift to low-osmolarity medium is also accompanied by a dramatic slowing of the overall rate of growth (mass increase) (47). We suspect that *ftsEX* contributes to both cell division and growth, but it has proven difficult to exclude the possibility that the growth defect is caused by attempts at cell division that go awry.

FtsEX contributes to cytokinesis by improving the assembly and/or stability of the septal ring. Septal ring assembly in an *ftsEX* mutant is fairly normal in LB that contains 1% NaCl but defective in LB that lacks NaCl (hereinafter referred to as LB0N) (47). More precisely, in LB0N, septal ring assemblies contain the "early" division proteins FtsZ, FtsA, and ZipA but lack the "late" proteins FtsK, FtsQ, FtsL, FtsI, and FtsN. The mechanism by which FtsEX contributes to septal ring assembly is still under investigation, but it probably involves protein-protein interactions, because FtsX has been shown to interact with FtsA and FtsQ in a bacterial two-hybrid system (31), while FtsE has been shown to interact with FtsZ in a coprecipitation assay (15). The FtsE-FtsZ interaction could be important for improving constriction rather than, or in addition to, septal ring assembly.

Remarkably, nothing is known about FtsEX's most obvious potential function—transporting a substrate involved in septum assembly. We are aware of only two studies that attempted to address this issue. The first concluded that FtsEX is needed for insertion of potassium transporters in the cytoplasmic membrane (54). However, in our view the data were not compelling and the connection to cell division, if any, is not obvious. The other study noted that *ftsE* and *ftsX* are cotranscribed with *ftsY*, which is a component of the signal recognition particle pathway for insertion of many proteins into the cytoplasmic membrane (20). That study therefore tested an *ftsEX* null mutant for defects in export of β-lactamase to the periplasm or insertion of leader peptidase into the cytoplasmic membrane. No such defects were found, so the authors concluded that FtsEX function is probably unrelated to FtsY. Besides these studies, at least one review article suggested that FtsEX might insert division proteins into the cytoplasmic membrane (8). Obviously, the finding that localization of several membrane proteins to the septal ring shows a leaky but pronounced dependence on FtsEX could be explained if the "missing" proteins were not getting into the membrane efficiently. Despite these speculations about potential FtsEX substrates, it is important to note that some members of the ABC "transporter"

* Corresponding author. Mailing address: Department of Microbiology, University of Iowa, 3-403 BSB, Iowa City, IA 52242. Phone: (319) 335-7785. Fax: (319) 335-9006. E-mail: david-weiss@uiowa.edu.

† Supplemental material for this article may be found at http://jb.asm.org/.

▽ Published ahead of print on 17 April 2009.

TABLE 1. Strains and plasmids

Strain or plasmid	Relevant feature(s)	Construction, source, or reference
Strains		
EC251	MG1655	Laboratory collection
EC436	MC4100 Δ(λ*attL-lom*)::(*bla lacI*^{q} P_{204}-*gfp-ftsI*)	58
EC437	MC4100 Δ(λ*attL-lom*)::(*bla lacI*^{q} P_{206}-*gfp-ftsI*)	This study
EC439	MC4100 Δ(λ*attL-lom*)::(*bla lacI*^{q} P_{206}-*gfp-ftsL*)	This study
EC441	MC4100 Δ(λ*attL-lom*)::(*bla lacI*^{q} P_{206}-*gfp-ftsN*)	This study
EC449	MC4100 Δ(λ*attL-lom*)::(*bla lacI*^{q} P_{206}-*ftsZ-gfp*)	This study
EC450	MC4100 Δ(λ*attL-lom*)::(*bla lacI*^{q} P_{206}-*zipA-gfp*)	58
EC452	MC4100 Δ(λ*attL-lom*)::(*bla lacI*^{q} P_{204}-*gfp*)	58
EC1068	MG1655 Δatt_{HK022}::(pAH144::P_{BAD}-*ftsEX*)	This study
EC1111	EC1068 Δ*ftsEX*::*cam*	This study
EC1117	EC1068 Δ*ftsEX*	This study
EC1215	EC251 Δ*ftsEX*	This study
EC1335	MG1655 *ftsE::kan*/pBAD33-*ftsEX*	47
EC1882	EC1215 Δ(λ*attL-lom*)::(*bla lacI*^{q} P_{204}::*gfp-ftsI*)	This study
KS272	Δ*lacX74*, *galE*, *galK*, *thi*, *rpsL*, Δ*phoA* (PvuII)	48
MC4100	*araD139*Δ*lacU169* Δ*relA19 rpsL150 thi mot flb-5301 deoC7 pstF25 rbsR*	Laboratory collection
Plasmid		
pAH144	CRIM plasmid, Spc^r	29
pBAD33	Arabinose regulation (P_{BAD}), p15A *ori*, Cam^r	28
pCP20	FLP recombinase, Amp^r Cam^r	13
pKD46	λ Red recombinase, Amp^r	18
pTH18-kr	IPTG-inducible (P_{lac}), Kan^r, pSC101 *ori*	30
pDSW438	pBAD33::*'phoA*	This study
pDSW439	pBAD33::*ftsI*$_{MSS}$-*'phoA* (first 81 codons of *ftsI* fused to *phoA*)	This study
pDSW513	*ftsX-gfp*, IPTG-inducible, Kan^r	47
pDSW525	pAH144::P_{BAD}::*ftsEX*, Spc^r	This study
pDSW609	pTH18-kr::*ftsE*–3×HA	47
pDSW610	pBAD33::*ftsEX*	47
pDSW621	pBAD33::*ftsX*	47
pDSW700	pBAD33::*ftsE*(*D162A*)*X*	This study
pDSW703	pBAD33::*ftsE*(*K41Q*)*X*	This study
pDSW712	pBAD33::*ftsE*(*E163A*)*X*	This study
pDSW890	pTH18-kr::*ftsE*(*K41Q*)–3×HA	This study
pDSW891	pTH18-kr::*ftsE*(*D162A*)–3×HA	This study
pDSW892	pTH18-kr::*ftsE*(*E163A*)–3×HA	This study
pDSW904	pTH18-kr::*ftsE*	This study
pDSW905	pTH18-kr::*ftsX*	This study
pDSW906	pTH18-kr::*ftsEX*	This study
pDSW907	pTH18-kr::*ftsE*(*K41Q*)*X*	This study
pDSW988	pTH18-kr::*ftsE*(*D162A*)*X*	This study
pDSW989	pTH18-kr::*ftsE*(*E163A*)*X*	This study

family do not move anything across cell membranes (reviewed in reference 19), so it cannot be taken for granted that FtsEX is a transporter at all.

MATERIALS AND METHODS

Media. LB consisted of 10 g of tryptone, 5 g of yeast extract, and 10 g NaCl per liter, with 15 g agar/liter for plates. For LB0N, the NaCl was omitted. Antibiotics were used at the following concentrations: chloramphenicol (Cam), 10 μg/ml; kanamycin (Kan), 40 μg/ml; ampicillin (Amp), 100 μg/ml for plasmids and 25 μg/ml for chromosomal alleles; and spectinomycin (Spc), 50 μg/ml. Isopropyl-β-D-thiogalactopyranoside (IPTG) was used at 0.1 mM, while L-arabinose (Ara) and D-glucose (Glu) were used at 0.2%. Cultures were grown at 30°C.

Bacterial strains. Strains and plasmids used in this study are listed in Table 1. Strains EC437, EC439, EC441, and EC449 were constructed from MC4100 using λ InCh as described previously (10, 58), except that the respective *fts* genes were initially cloned into pDSW209 or pDSW210. EC1215, a markerless *ftsEX* deletion mutant derived from MG1655, was constructed in several steps. First, a complementing copy of *ftsEX* was introduced into EC251 (our laboratory's isolate of MG1655) by transformation with the CRIM helper plasmid pAH69 followed by integration of the CRIM plasmid pDSW525 (Spc^r, pAH144::P_{BAD}::*ftsEX*) into the chromosome at the HK022 *att* site to produce EC1068 (29). Second, the authentic copy of *ftsEX* in the 76-min region was replaced with a Cam^r marker using λ Red methods (18). To do this, an 1,114-bp Δ*ftsEX*::Cam fragment was obtained by PCR on the Cam^r template plasmid pKD3 using P494 (AGAGGCACTTTTTGCCCGAGAGGATTAA CAATGATTCGCTTTGAACATGTGTGTAGGCTGGAGCTGCTTC) and P495 (ATCAAACTTCGTTCCGAAAACCTGTGCCACTTCCGCAACCG CCGATGACACATATGAATATCCTCCTTAG) as primers. This fragment was used to replace *ftsEX* in EC1068/pKD46 (carries λ Red recombinase). Recombinants were selected on LB Cam Ara; the arabinose serves to induce P_{BAD}::*ftsEX* and was maintained in all subsequent steps. Recombinants were confirmed by colony PCR using the primers C1 and C2, described in reference 18, along with the gene-specific primers P505 (GCCTGCAGAACAAA TCGCACC) and P506 (GACATAGAGATGAAATACCGG). An isolate with the desired deletion of *ftsEX* was saved as EC1111. Third, the FLP recombinase plasmid pCP20 (13) was used to excise the Cam marker, creating EC1117. Finally, the complementing P_{BAD}::*ftsEX* was evicted using pAH83 (29) to create EC1215. The deletion in EC1215 extends from codon 6 of *ftsE* to codon 297 of *ftsX* and does not disrupt the major promoter for *rpoH* embedded in the 3′ end of *ftsX* (22). To create EC1882, EC1215/pDSW610 was transduced to Amp^r with P1 phage grown on EC436.

Molecular biological procedures and oligonucleotides. Standard procedures for cloning and analysis of DNA, PCR, electroporation, and transformation were used (5). Kits from Qiagen (Valencia, CA) were used to isolate DNA. Enzymes used to manipulate DNA were from New England Biolabs (Beverly, MA).

Oligonucleotides were from Integrated DNA Technologies (Coralville, IA). Sequencing of DNA was performed by the DNA Core Facility of the University of Iowa using dye terminator cycle-sequencing chemistry. All constructs made by PCR were sequenced to verify their integrity.

Site-directed mutagenesis and plasmids. Megapriming (46) was used to introduce lesions into the ATP-binding site of *ftsE* in the plasmid pDSW610, a pBAD33 derivative that carries wild-type *ftsEX* (28, 47). The *ftsE*(*K41Q*) mutation was introduced by PCR with the primers P629 (GGCGGATCCATTCGC TTTGAACATGTC) and P657 (CAGCTTCAGGAGGGTACTTTGCCCTGC GCCGGAATGACCG), using pDSW610 as a template. The resulting 147-bp PCR product was purified by agarose gel electrophoresis and used as a megaprimer together with P630 (GCGAAGCTTTTATTCATGGCCCACGCC) to PCR-amplify *ftsE* from pDSW610. This produced a 684-bp fragment that was digested with PstI and SphI; these sites are internal to the PCR fragment rather than encoded by the primers. Finally, the restriction fragment was ligated into PstI/SphI-digested pDSW610 to create pDSW703 (P_{BAD}::*ftsE*(*K41Q*)*X*). Plasmid pDSW700 (P_{BAD}::*ftsE*(*D162A*)*X*) was constructed similarly except that the primers used to make the megaprimer were P652 (CGGGATCCTCATCGTG AACCTCGTAC) and P630. The resulting megaprimer was used together with P629 to create an *ftsE*(*D162A*) PCR fragment that was cloned into PstI/SphI-digested pDSW610. Plasmid pDSW712 (P_{BAD}::*ftsE*(*E163A*)*X*) was constructed using P629 and P720 (CCAGGTTACCAGTCGGTGCGTCCGCCAGCAG) to make the megaprimer, which was then used together with P632 (GCGAAGCT TTTATTCAGGCGTAAAGTGG) to make a longer PCR product that was used to replace the 1,663-bp PstI-HindIII fragment of pDSW610.

Plasmid pDSW609 is derived from pTH18-kr (copy number, ~5) and carries P_{lac}::*ftsE*–3×HA (30, 47). To construct derivatives that fused a 3× hemagglutinin (HA) tag (3×HA) to *ftsE* alleles with ATP-binding site mutations, the 565-bp PstI-SphI fragment of pDSW609 was replaced with the corresponding fragment from pDSW700, pDSW703, and pDSW712. A derivative that lacks the 3×HA tag was constructed by PCR amplification of *ftsE* with its stop codon from pDSW610 using P629 and P630 as primers. The 684-bp product was cut with PstI and HindIII and ligated into the same sites of pDSW609 to create pDSW904 (P_{lac}::*ftsE*). It should be noted that the 3× HA tag was removed by the PstI-HindIII digestion. A derivative that expresses *ftsE* and *ftsX* with their authentic coupling (the first 7 bp of *ftsX* overlap the 3′ end of *ftsE*) was created by subcloning the 1,663-bp PstI-HindIII fragment carrying *ftsE* and *ftsX* from pDSW610 into the same sites of pDSW609 to create pDSW906 (P_{lac}::*ftsEX*). Derivatives of *ftsE* that encode the K41Q, D162A, and E163A lesions were created similarly from pDSW703, pDSW700, and pDSW712, respectively. These plasmids are pDSW907 [P_{lac}::*ftsE*(*K41Q*)*X*], pDSW988 [P_{lac}::*ftsE*(*D162A*)*X*], and pDSW989 [P_{lac}::*ftsE*(*E163A*)*X*]. A derivative that expresses only *ftsX* was created by PCR amplification of *ftsX* from pDSW610 using the primers P911 (GGCGA ATTCAAATAAGCGCGATGCAATCAATC) and P632. The 1,073-bp product was cut with EcoRI and HindIII and then ligated into the same sites of pDSW609 to create pDSW905 (P_{lac}::*ftsX*).

The *phoA* fusions used to determine the topology of FtsX were constructed by PCR methods. Briefly, a *′phoA* fragment that encodes most of *phoA* was cloned into pBAD33 to create pDSW438. PhoA fusions were then constructed by PCR amplification of fragments of *ftsX* of various lengths, using a common 5′ primer (P686) and any of several 3′ primers (see Table S1 in the supplemental material). PCR products were digested with SacI (cuts in the 5′ primer) and either StuI or ScaI (cut in the 3′ primers), both of which generate blunt ends. The *ftsX′* fragments were ligated into pDSW438 that had been digested with SacI and StuI. The 3′ primers and resulting fusion sites in FtsX are as follows: P688 (R47), P689 (S69), P690 (S108), P691 (R145), P692 (S187), P693 (R213), P694 (R245), P695 (R270), P696 (R297), P697 (S300), and P698 (E352). A positive-control *ftsI′-′phoA* fusion was constructed by PCR amplification of the first 81 codons of *ftsI*; this product was digested with SacI and StuI and then ligated into the same sites of pDSW438 to create pDSW439.

General microscopy methods. Our microscope, camera, and software have been described previously (39, 59). Where indicated, nucleoids were stained with 4′,6-diamidino-2-phenylindole from Vector Laboratories (Burlingame, CA) and membranes were stained with FM4-64 [*N*-(3-triethylammoniumpropyl)-4-(6-(4-(diethyl-amino)phenyl)hexatrienyl) pyridinium dibromide] from Molecular Probes (Eugene, OR). Digital images were imported to the Adobe Photoshop software program for cropping and minor adjustments to brightness and contrast. Final figures were assembled in Canvas. Depending on the experiment, cells were either fixed with formaldehyde-glutaraldehyde (42) or methanol (49) or live cells were immobilized on an agarose pad and photographed without fixation. For microscopy of live cells, slides were prepared by pipetting 40 μl of molten 1% agarose (in water) onto a prewarmed glass slide with two spacers made of laboratory tape. A second glass slide was placed on top to create a thin agarose pad. Once cooled, the two slides were separated and 5 μl of live culture in growth medium was applied to the agarose pad and covered with a no. 1 coverslip.

Western blotting. Western blotting was done essentially as described previously (58). Primary antibodies against FtsE–3×HA and PhoA fusions were monoclonal HA.11 (BabCo, Berkeley, CA) and polyclonal anti-PhoA (5 Prime→3 Prime, Boulder, CO), respectively. Anti-FtsK, anti-FtsQ, anti-FtsI, and anti-FtsN were all polyclonal antibodies raised in rabbits and have been described previously (12, 56, 58, 59). Secondary antibodies were from Pierce (Rockford, IL) and were conjugated to horseradish peroxidase. Blots were developed with chemiluminescent substrates and visualized with an LAS1000 imager from Fuji (Stamford, CT).

Testing effect of FtsEX depletion on levels of Fts membrane proteins. Strain EC1335 was grown in LB0N containing either Glu or Ara as described previously (47), except that the culture volume was increased to 500 ml. After about 5 h, cells in the glucose culture were ~20 μm long while those in the arabinose culture were ~5 μm long. Cells were harvested by centrifugation, resuspended in 2.5 ml of Tris-NaCl buffer (50 mM Tris, 50 mM NaCl, pH 8.0), and stored frozen at −80°C. For lysis, cells were thawed and EDTA and lysozyme were added to final concentrations of 5 mM and 0.1 mg/ml, respectively. Then, Benzonase (Novagen, Madison, WI) and protease inhibitor cocktail set V (Calbiochem, La Jolla, CA) were added, and samples were incubated on ice for 30 min. Lysis was completed by sonication. The lysate was centrifuged for 10 min at 8,000 × *g* to remove debris. The resulting supernatant was termed the crude extract, and a sample was saved for analysis by Western blotting. The remainder was centrifuged at 100,000 × *g* for 75 min. The supernatant was saved as the soluble fraction, while the pellet was resuspended in 0.4 ml of Tris-NaCl buffer and considered the membrane fraction. A Bradford assay was used to determine the protein levels in all three fractions, with bovine serum albumin as a standard. Ten μg of protein from each fraction were subjected to sodium dodecyl sulfate-polyacrylamide gel electrophoresis and Western blotting to determine levels of FtsK, FtsQ, FtsI, and FtsN.

Complementation assays. EC1215 transformants harboring pTH18kr-based plasmids (including the positive and negative controls, pDSW906 and TH18-kr) were grown overnight in LB with Kan (LB Kan) containing glucose to reduce leaky expression. To test the efficiency of colony formation, overnight cultures were adjusted to 10^9 cells/ml and serial dilutions were spotted onto LB and LB0N plates containing Kan and IPTG (LB Kan IPTG and LBDN Kan IPTG). Plates were incubated at 30°C for 18 h before photography. To test the ability of the mutant proteins to support growth and cell division upon a shift to LB0N, log-phase cultures (optical density at 600 nm [OD_{600}], ~0.8) growing in LB Kan were diluted 10-fold into LB Kan IPTG or LB0N Kan IPTG. Growth was monitored by measuring the OD_{600}, and cell morphology was monitored by phase-contrast microscopy. The mean number of cell division events during the first 120 min after the shift to LB0N was calculated under the assumption that growth (mass increase) was exponential using the following relationship: $N = \log_2 \{(e[\ln(2) \times 120 \text{ min}/G])(L_{\text{time0}}/L_{\text{time120}})\}$. Here, N is the mean number of division events, ln is the natural logarithm, G is the mass doubling time in minutes, and L is the average cell length.

Localization of FtsE proteins with ATP-binding site lesions. Transformants that produced the FtsE–3×HA derivatives from low-copy-number plasmids were grown in LB or LB0N containing Kan and IPTG to an OD_{600} of ~0.3. A sample was taken to determine protein levels by Western blotting, and a second sample was fixed with methanol and processed for immunofluorescence microscopy using anti-HA antibody as described previously (47).

Effect of FtsE(D162A) on localization of Fts proteins in wild-type background. Cultures in exponential growth (OD_{600} of ~0.5) in LB Kan were induced by diluting them 1:50 into LB Kan IPTG. After 3 h of further growth, cells were fixed with formaldehyde-glutaraldehyde and the various green fluorescent protein (GFP)-Fts protein fusions were visualized by fluorescence microscopy.

Ability of mutant FtsE proteins to recruit FtsI and FtsN to septal rings. (i) For GFP-FtsI, these experiments used an FtsEX depletion strain designated EC1882 [Δ*ftsEX* P_{204}::*gfp-ftsI*/pDSW610(P_{BAD}::*ftsEX*)] carrying various pTH18-kr derivatives that express alleles of *ftsE* along with wild-type *ftsX* under the control of P_{lac}. Cultures were grown overnight in LB Kan Cam Ara. The next morning, cultures were diluted about 500-fold (to achieve a starting OD_{600} of 0.005) in LB0N Kan Cam with either Glu or Ara, which allows for depletion or maintenance of FtsEX production, respectively. After 2 h of growth, IPTG was added to induce chromosomal *gfp-ftsI* and plasmid-borne *ftsEX* constructs. Growth was continued for another 4 to 5 h, by which time the OD_{600} was ~0.4 and cells depleted of FtsEX were ~30 μm long. Live cells were then immobilized on an agarose pad and photographed. (ii) For FtsN and FtsZ, the *ftsEX* null strain

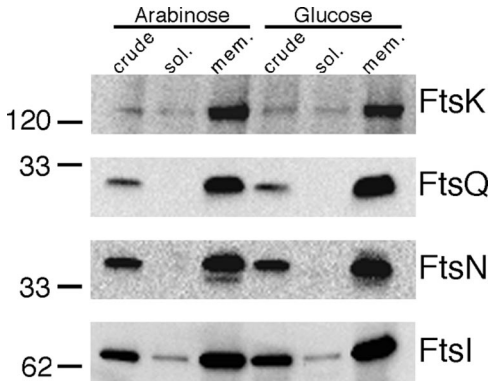

FIG. 1. Steady-state levels of Fts membrane proteins in cells depleted of FtsEX. The FtsEX depletion strain EC1335 was grown in LB0N Cam and either Ara or Glu for about 5 h, at which time the Glu culture was filamentous. Cells were fractionated, and FtsK, FtsQ, FtsN, or FtsI was detected by Western blotting. Only the relevant portion of each blot is shown. The position of a molecular mass marker and the protein detected are indicated to the left and right, respectively, of each blot. crude, crude extract; sol., soluble fraction; mem., membrane fraction.

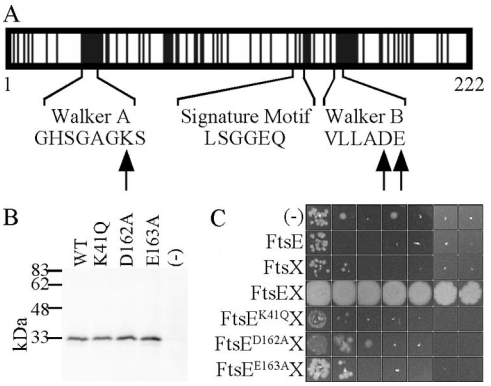

FIG. 2. ATP-binding site mutants of *ftsE*. (A) Cartoon of FtsE. Vertical black bars indicate invariant residues in an alignment of FtsE proteins from *E. coli*, *Salmonella enterica* serovar Typhimurium, *Yersinia pestis*, *Vibrio cholerae*, *Haemophilus influenzae*, *Pseudomonas aeruginosa*, and *Pasteurella multocida*. Sequences of the Walker A, Walker B, and ABC signature motifs are shown below, with residues targeted for mutagenesis indicated by arrows. (B) Steady-state level of mutant FtsE proteins. Strain EC251 (wild type) transformed with plasmids that direct expression of *ftsE*–3×HA alleles was induced with 0.1 mM IPTG, and whole cells were analyzed by Western blotting with anti-HA antibody. The location of molecular mass markers is shown at the left. FtsE-3×HA is predicted to be 28.5 kDa. The plasmids used were pDSW609, pDSW890, pDSW891, pDSW892, and pTH18-kr. (C) Complementation test. The Δ*ftsEX* null mutant EC1215 was transformed with low-copy-number P_{lac}::*ftsEX* plasmids (or controls) that direct production of the indicated proteins. Transformants were grown overnight in LB Kan, adjusted to 10^9 CFU/ml in LB0N, and 10-fold serial dilutions were spotted onto LB0N Kan with 0.1 mM IPTG. Plates were incubated overnight at 37°C and then photographed. The plating efficiency was ~100% for all strains when plates contained LB rather than LB0N (not shown). The plasmids used were pTH18-kr, pDSW904, pDSW905, pDSW906, pDSW907, pDSW988, and pDSW989.

EC1215 carrying pTH18-kr derivatives was grown overnight in LB Kan with glucose to limit leaky expression from the plasmids. The next morning, cultures were diluted 1:50 into LB Kan IPTG (except that in the case of *ftsE*(*D162A*), the IPTG was omitted until the next step). These cultures were grown to midlog phase and then diluted 10-fold into LB Kan IPTG or LB0N Kan IPTG. After 2 to 3 h of further growth, the OD_{600} was ~0.3, and cells were fixed and processed for immunolocalization of FtsN or FtsZ as described previously (42, 59).

Ability of FtsE and FtsX to localize independently of each other. To localize FtsX-GFP in the absence of FtsE, the *ftsEX* null strain EC1215 harboring pDSW513 (P_{204}::*ftsX-gfp*) was grown in LB Kan IPTG to an OD_{600} of ~0.8, diluted 10-fold into the same medium with or without NaCl, and grown for 2 to 3 h. Fluorescence microscopy was used to visualize GFP in both live and formaldehyde-glutaraldehyde-fixed cells. Localization of FtsE was tested similarly using a plasmid that expresses 3×HA-tagged FtsE. Cells were fixed with methanol, and FtsE was detected with anti-HA antibody (47).

Computer-predicted topology of FtsX. The following programs were used with default parameters to predict the membrane topology of FtsX: TopPred (http://bioweb.pasteur.fr/seqanal/interfaces/toppred.html), TMPred (http://www.ch.embnet.org/software/TMPRED_form.html), HMMTOP (http://www.enzim.hu/hmmtop/html/submit.html), and TMHMM (http://www.cbs.dtu.dk/services/TMHMM-2.0/) (14, 36, 53).

Alkaline phosphatase assay. Strain KS272 is *phoA* minus and was used as the host strain to determine the topology of FtsX. Overnight cultures grown in LB Cam were subcultured 1:100 into 5 ml of the same medium and grown for 3 h before 70 μl of 20% arabinose solution was added to induce expression of the *phoA* fusions. Samples were taken 1 h after induction, and alkaline phosphatase activity was determined as described previously (38). All constructs were assayed in three independent experiments in duplicate. Samples were also taken for Western blotting analysis to determine the steady-state level of the PhoA fusion protein.

RESULTS

FtsEX does not transport Fts proteins into the cytoplasmic membrane. We demonstrated previously that several proteins needed for cell division in *E. coli* localize poorly to the septal ring when cells growing in LB0N medium are depleted of FtsEX (47). Among these proteins are FtsK, FtsQ, FtsI, and FtsN—all of which reside in the cytoplasmic membrane (9, 11, 16, 21). To determine whether insertion of these division proteins into the membrane depends on FtsEX, we used a previously described depletion strain named EC1335 that expresses *ftsEX* from an arabinose-inducible pBAD plasmid (47). Cells were grown in LB0N containing arabinose or glucose until the latter were filamentous; average cell lengths at time of harvest were ~5 μm and ~20 μm for the arabinose and glucose cultures, respectively. Then, cells were fractionated and examined by Western blotting with polyclonal antibodies against FtsK, FtsQ, FtsI, and FtsN. Depletion of FtsEX did not have any obvious effect on the abundance of any of the four proteins examined (Fig. 1), despite the fact that division had essentially ceased in the depleted cells. This finding argues that FtsEX does not insert any of the proteins we studied into the cytoplasmic membrane.

Mutant FtsE proteins with lesions in the ATP-binding motifs. Site-directed mutagenesis was used to introduce amino acid substitutions into the Walker A (K41Q) or Walker B (D162A, E163A) ATP-binding motifs (Fig. 2A). Similar lesions have been made in numerous other ABC transporters. Based on this literature, the K41Q and D162A mutant proteins are not expected to bind ATP, while the E163A protein should bind ATP but not hydrolyze (see reference 19 and references therein). However, the literature on ABC transporters is enormous, and not all published reports are consistent with these predictions or each other. We attempted to characterize the ATP-binding properties of our mutant proteins but encoun-

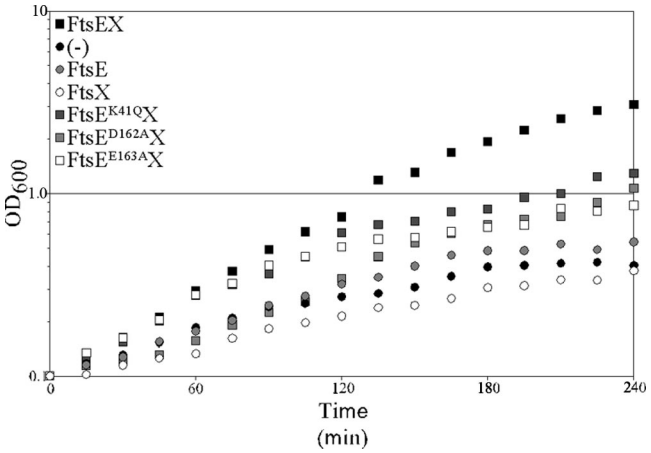

FIG. 3. Effect of ATP-binding site lesions in FtsE on growth in LB0N. Cultures of the Δ*ftsEX* null mutant EC1215 carrying various *ftsEX* plasmids (or controls) were grown to mid-log phase in LB Kan with 0.1 mM IPTG. At time zero, these cultures were diluted into LB0N Kan with 0.1 mM IPTG. The plasmids used were pTH18-kr (black circles), pDSW904 (medium-gray circles), pDSW905 (open circles), pDSW906 (black squares), pDSW907 (dark-gray squares), pDSW988 (light-gray squares), and pDSW989 (open squares).

tered severe problems with solubility of FtsE, and this line of investigation was abandoned.

The mutant *ftsE* alleles were fused to three tandem copies of the hemagglutinin epitope tag (3×HA) and expressed from a low-copy-number plasmid with an IPTG-inducible P_{lac} promoter. We demonstrated previously that wild-type FtsE–3×HA localizes to the septal ring and supports cell division (47). Western blotting of whole-cell extracts with anti-HA antibody revealed that all three mutant FtsE proteins were produced at levels comparable to that of the wild type (Fig. 2B).

Phenotype of *ftsE* ATP-binding site mutants. We tested the ability of our mutant FtsE proteins to rescue the growth, division, and viability of an *ftsEX* null mutant in LB0N. To this end, we constructed a set of low-copy-number P_{lac} plasmids that express both *ftsE* and *ftsX*, preserving the normal 7-bp overlap of these genes but omitting the 3×HA tag from *ftsE*. We also constructed a new *ftsEX* null mutant, named EC1215, that has a markerless deletion extending from codon 6 of *ftsE* to codon 297 of *ftsX*. This deletion leaves intact the major promoter for σ^{32} embedded in the 3′ end of *ftsX* (22). We constructed EC1215 because the mutant used in our previous study, RG60, has a nonexcisable Kan^r determinant in *ftsE*, making it incompatible with our P_{lac}::*ftsEX* plasmids, which confer Kan^r (20, 47). Phenotypically EC1215 is indistinguishable from RG60. By way of clarification, it should be noted that RG60 was originally reported to be rescued by electrolytes but not osmolytes (20). However, Reddy subsequently demonstrated that both electrolytes and osmolytes rescue an independently constructed *ftsEX* null mutant (44). We reinvestigated this issue and found that RG60 and EC1215 are both rescued by osmolytes (data not shown), so osmotic rescue of *E. coli ftsEX* null mutants is a general phenomenon.

To test the functionality of the FtsE proteins with ATP-binding site lesions, EC1215 transformants were grown in LB and then transferred to LB0N. The results are summarized in Fig. 3 and Table 2.

Transferring the null mutant (EC1215/P_{lac} vector) to LB0N caused a sudden and dramatic slowing of growth. Prior to the shift, the mass doubling time was 40 min and the average cell length was ~12 μm. During the first 120 min postshift, the mass doubling time was ~70 min and the average cell length increased to ~17 μm. The modest increase in cell length reflects both the low rate of growth and the leakiness of the division defect, since each cell divided ~1 time during the first 2 h in LB0N. For comparison, the wild type (EC1215/P_{lac}::*ftsE*^{WT}*X*) grew with a doubling time of ~40 min in LB0N and divided three times during 2 h. While the K41Q and E163A mutant proteins rescued growth in the sense of mass increase (doubling times, ~50 min), the D162A protein did not (doubling time, ~80 min), and none of the three mutant proteins rescued cell division (~1 division event in 2 h, comparable to results for the empty vector control). As a result, all three transformants (EC1215/P_{lac}::*ftsE*^{mut}*X*) became ~16 μm long during the first 2 h after the shift to LB0N, only slightly shorter than the empty vector

TABLE 2. Growth and division of *ftsE* mutants in LB and LB0N[a]

Plasmid carrying:	Result with medium[b]						Plating efficiency (%)[g]
	LB		LB0N				
	Avg length (μm)[c]	Doubling time (min)[d]	Avg length (μm)[c]	Doubling time (min)[d]	No. of division events[e]	% Sick cells[f]	
ftsE^{WT}*X*	4.1	40	4.4	39	3.0	1	100
(−)	11.5	40	17.0	72	1.1	66	0.0001
ftsE	9.5	38	16.5	67	1.0	70	0.0001
ftsX	9.9	41	16.4	84	0.7	63	0.0001
ftsE(K41Q)X	8.4	40	16.5	49	1.5	41	0.001
ftsE(D162A)X	11.2	38	16.4	84	0.9	49	0.001
ftsE(E163A)X	5.5	40	15.8	50	0.9	55	0.001

[a] All data are averages for two independent experiments in which the values agreed to within 10%. The strains used are listed in the legend to Fig. 3. (−), empty vector.
[b] Values in LB are steady state, but values in LB0N refer to the first 120 min postshift unless noted otherwise.
[c] Based on measurements of at least 100 cells in each of two experiments.
[d] Mass increase as determined by OD_{600}.
[e] No. of times the average cell divided as calculated using the formula described in Materials and Methods.
[f] Determined by phase-contrast microscopy and DAPI staining 5 h after the shift.
[g] Control experiments confirmed that all strains had ~100% viability on plates that contained NaCl (i.e., LB Kan IPTG).

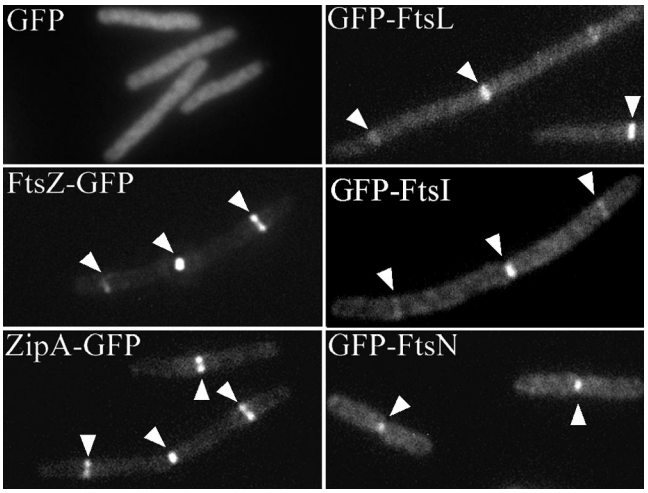

FIG. 4. Effect of FtsE(D162A) on cell division and septal ring assembly. Wild-type cells expressing both the indicated *gfp* construct and *ftsE*(*D162A*) (together with *ftsX*) were fixed, and GFP was visualized by fluorescence microscopy. Arrows indicate sites of Fts protein localization. The strains shown are EC437 (*gfp-ftsI*), EC439 (*gfp-ftsL*), EC441 (*gfp-ftsN*), EC449 (*ftsZ-gfp*), EC450 (*zipA-gfp*), and EC452 (*gfp*). All carry plasmid pDSW988 (P_{lac}::*ftsE*(*D162A*)*X*).

control (~17 μm). By 5 h postshift, growth had essentially stopped and about half of the cells appeared to be dead as judged by phase-contrast microscopy and 4′,6-diamidino-2-phenylindole staining, which revealed many ghost cells and gross defects in nucleoid structure. Consistent with this, the plating efficiency of EC1215/P_{lac}::*ftsE*^{mut}*X* on LB0N was ~0.001% (Fig. 2C), and even this value is probably too high, because restreaking revealed that most of the colonies obtained had acquired suppressor mutations. Efforts to find conditions of salt and temperature under which the ATP-binding site mutant proteins rescued colony formation compared to that for an empty vector control were unsuccessful.

FtsE(D162A) is a mild dominant negative that impairs constriction of the septal ring in wild-type *E. coli*. Although none of the mutant FtsE proteins studied here were strong dominant negatives, the D162A mutant protein impaired cell division modestly when produced in a wild-type background. We therefore transformed the low-copy-number P_{lac}::*ftsE*(*D162A*)*X* plasmid into a set of wild-type strains that harbored chromosomal *gfp* fusions to various division genes. Production of FtsE(D162A) increased the proportion of cells in the population with septal rings containing the late division proteins FtsL or FtsI from about ~50% to about ~95%, and we readily observed filamentous cells with multiple septal rings (Fig. 4; see Table S2 in the supplemental material). The fraction of cells exhibiting septal GFP-FtsN also increased, in this case from ~40% to ~60%, but long cells with multiple sites of GFP-FtsN localization were not observed because GFP-FtsN suppressed the dominant-negative effect of FtsE(D162A) (compare length of GFP-FtsN to that of the GFP control in Table S2 in the supplemental material). Similar overproduction of wild-type FtsE was not deleterious to division and had little or no effect on Fts protein localization (see Table S2 in the supplemental material). Taken together, these findings imply FtsE(D162A) inhibits division at a step after septal ring assembly.

FtsE proteins with ATP-binding site lesions localize to septal rings. Our observations concerning the dominant-negative effect of FtsE(D162A) suggested that FtsE uses ATP to promote septal ring constriction rather than septal ring assembly. They also suggested that the mutant protein assembles into the septal ring. If it had blocked division by mislocalizing, it should have sequestered other Fts proteins away from the septal ring, which was not the case.

To examine localization of the mutant FtsE proteins directly, we fused them to a C-terminal 3×HA tag and produced them from a low-copy-number P_{lac} plasmid in both a wild-type and Δ*ftsEX* null mutant background. Because FtsE localization depends upon FtsX (see below), when working with the Δ*ftsEX* strain, we supplied FtsX from a compatible P_{BAD} plasmid. Transformants were grown with inducers in LB and LB0N and then fixed and processed for immunofluorescence microscopy with anti-HA antibody. All three mutant forms of FtsE localized to septal rings in both the wild type (not shown) and a Δ*ftsEX* null mutant (Fig. 5; Table 3) grown with or without NaCl.

FtsE ATP-binding site mutants support recruitment of FtsI and FtsN to septal rings. The finding that mutant FtsE proteins localize to the septal ring led us to ask whether they support recruitment of downstream division proteins. To test this hypothesis, we examined recruitment of the last two essential proteins in the recruitment hierarchy, FtsI and FtsN (3, 58), since their presence would imply septal rings are complete.

We lack good enough antibodies against FtsI to localize it by immunofluorescence, so we used a chromosomal *gfp-ftsI* fusion instead. This, however, was not without its own set of challenges, because in our hands, *ftsEX* null strains do not tolerate expression of *gfp-ftsI*, which is surprising given that the *gfp-ftsI* fusion is functional as assessed by complementation (58). For these reasons, we used an FtsEX depletion background that expresses wild-type *ftsEX* from an arabinose-inducible P_{BAD} plasmid and *gfp-ftsI* from an IPTG-inducible chromosomal gene. The *ftsE* allele to be tested was introduced (together with *ftsX*) on an IPTG-inducible P_{lac}::*ftsEX* plasmid. Strains were grown in LB0N containing glucose and IPTG until the P_{lac} empty vector control became filamentous and live cells were visualized by fluorescence microscopy (Fig. 6 and Table 4).

Because the leaky dependence of FtsI on FtsEX makes these results somewhat complex, we will describe them in detail, starting with the positive and negative controls. When the depletion strain was grown in the presence of glucose but a complementing P_{lac}::*ftsEX* plasmid was induced, cells averaged ~9 μm in length, ~75% exhibited at least one septal ring containing GFP-FtsI, and the frequency of GFP-FtsI rings when normalized to cell length (a proxy for mass) was ~1 per 11 μm. In the negative control, which carried a P_{lac} empty vector, depletion of FtsEX increased the cell length to ~30 μm but only ~45% of these filaments had a septal ring containing GFP-FtsI, and the frequency of GFP-FtsI rings was ~1 per 40 μm. These results are similar to those we observed previously using different strains (47).

When cells depleted of FtsEX contained either the P_{lac}::*ftsE* or P_{lac}::*ftsX* plasmid, the results were essentially identical to those observed with an empty P_{lac} vector, namely, filamentous

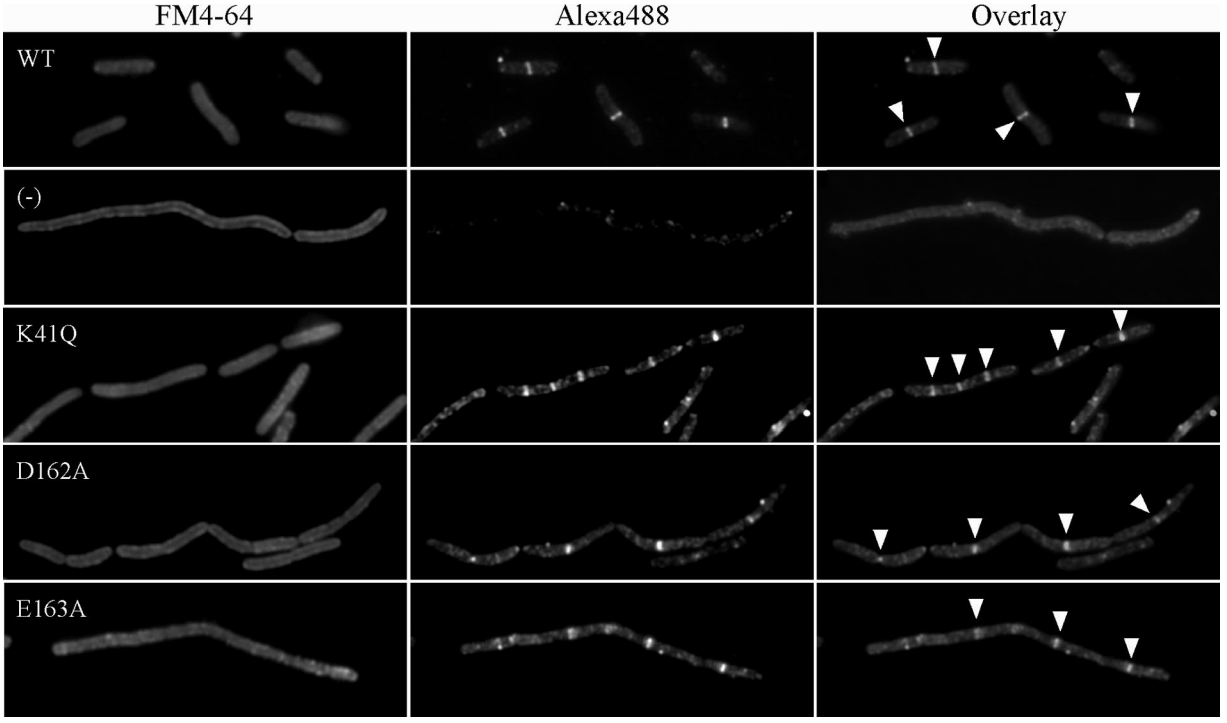

FIG. 5. ATP-binding site mutants of FtsE localize to potential division sites. EC1215 (Δ*ftsEX*) cotransformed with plasmids that express *ftsX* (pDSW621) and the indicated *ftsE*–3×HA allele (pDSW609, pTH18-kr [(−)], pDSW890, pDSW891, or pDSW892) were grown in LB0N containing antibiotics, Ara (to induce *ftsX*), and 0.1 mM IPTG (to induce *ftsE*). Cells were fixed, and FtsE was visualized by immunofluorescence microscopy, with a secondary antibody conjugated to Alexa 488 used to detect FtsE-3×HA. Membranes were stained with FM4-64. Arrows indicate sites of FtsE localization.

cells with ~1 GFP-FtsI band per 45 μm. This implies that an FtsEX complex is needed for recruitment of downstream proteins to the septal ring. Notably, producing an FtsE ATP-binding site mutant protein together with FtsX largely restored GFP-FtsI localization, implying that FtsE probably does not have to bind and hydrolyze ATP to fulfill its function in septal ring assembly. For example, comparing P_{lac}::*ftsX* to any of the three P_{lac}::*ftsE*^{mut}*X* plasmids showed that an FtsE protein with an ATP-binding site lesion increased the fraction of filaments with at least one GFP-FtsI ring from ~40% to ~80% and increased the frequency of rings from ~1 per 45 μm to ~1 per 15 μm. This two- to threefold improvement in GFP-FtsI localization was not associated with a comparable improvement in division, since the filaments averaged ~30 μm and ~26 μm with P_{lac}::*ftsX* and P_{lac}::*ftsE*^{mut}*X*, respectively. Although the ring spacing with P_{lac}::*ftsE*^{mut}*X* was not as good as that observed with P_{lac}::*ftsEX* (15 μm versus 11 μm), we think this modest defect is an indirect effect of filamentation (see below).

To study FtsN localization, we transformed our set of P_{lac} plasmids into an *ftsEX* null strain and visualized the endogenous FtsN protein by immunofluorescence microscopy. Filaments obtained from the null mutant in this experiment were shorter than those obtained from the depletion strain used for GFP-FtsI because the null mutant became sick and grew poorly

TABLE 3. Localization of FtsE proteins with a mutant ATP-binding site[a]

Characteristic of FtsE protein	Presence of NaCl	No. of cells	Length[b] (μm)	No. of rings	% Cells with ring(s)	Ring spacing[c] (μm)
Wild type	+	227	3.8 (1.8)	112	49	7.7
	−	333	5.2 (2.2)	257	74	6.7
None	+	206	5.8 (2.8)	0	0	>1,200
	−	167	13.5 (8.7)	2	1	1,100
K41Q	+	243	5.0 (2.8)	155	60	7.8
	−	154	13.8 (7.0)	156	65	14
D162A	+	166	4.9 (2.0)	83	49	9.8
	−	206	14.2 (9.2)	201	61	15
E163A	+	86	5.1 (1.9)	48	53	9.1
	−	120	13.8 (8.7)	160	78	10

[a] Strains are derivatives of EC1215 (Δ*ftsEX*)/pBAD33::*ftsX* carrying the pTH18-kr derivatives listed in the legend to Fig. 5.
[b] Mean (standard deviation).
[c] (No. of cells × length)/no. of rings.

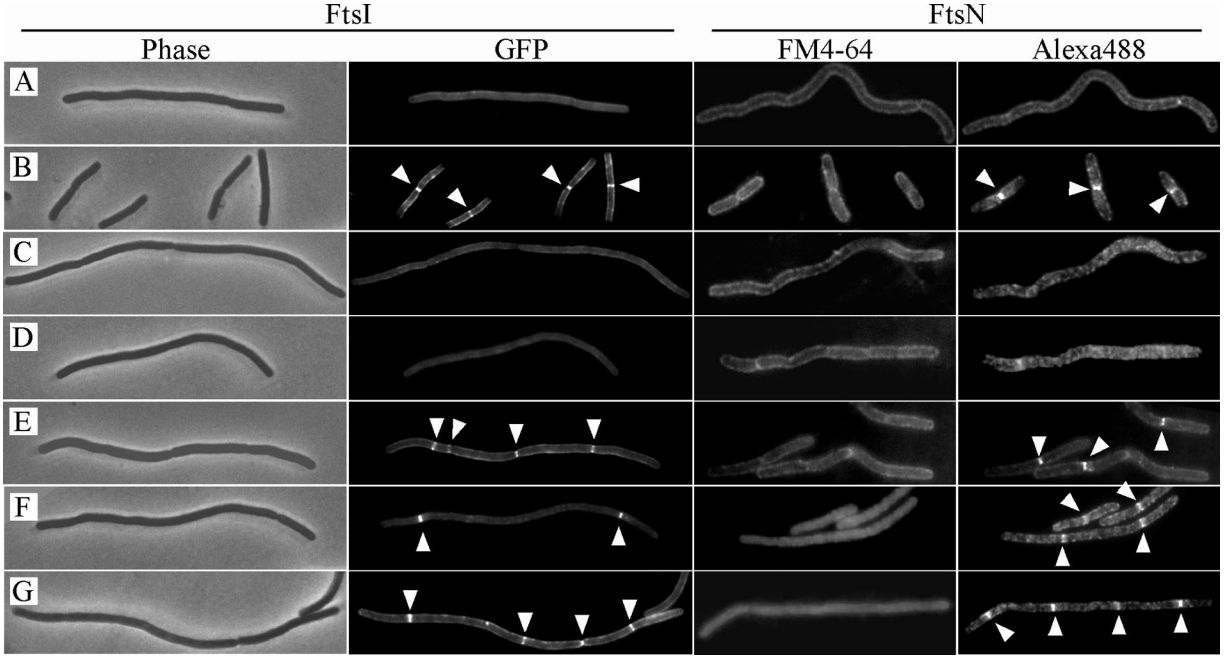

FIG. 6. ATP-binding site mutants of FtsE support recruitment of FtsI and FtsN to septal rings. Left panel set: localization of GFP-FtsI. Cells were fixed and photographed under phase-contrast and fluorescence microscopy. Arrows indicate sites of GFP-FtsI localization. The cells shown are derivatives of EC1882 carrying plasmids pTH18-kr (empty vector), pDSW906 (*ftsEX*), pDSW904 (*ftsE* alone), pDSW905 (*ftsX* alone), pDSW907 [*ftsE*(*K41Q*) and *ftsX*], pDSW988 [*ftsE*(*D162A*) and *ftsX*], and pDSW989 [*ftsE*(*E163A*) and *ftsX*] in rows A to G, respectively. Right panel set: localization of FtsN. Cells were fixed, processed for immunofluorescence microscopy to visualize FtsN, and stained with FM4-64 to visualize membranes. Arrows indicate sites of FtsN localization. The cells shown are derivatives of EC1215 carrying the same plasmids used to study GFP-FtsI recruitment in the left panel set.

after the shift to LB0N (Fig. 2) (47); sickness was especially an issue when the null mutant expressed *ftsE*(*D162A*), which had to be induced for a shorter period of time than the other mutant *ftsE* alleles. Nevertheless, the results for FtsN were analogous to the results for GFP-FtsI. FtsN localization exhibited a leaky but marked dependence on FtsEX, with ~1 band per 9 μm in the positive control (P_{lac}::*ftsEX*) compared to ~1 per 35 μm in the negative control (P_{lac} vector). Neither FtsE alone nor FtsX alone rescued localization of FtsN, but any of the three ATP-binding site mutants of FtsE could substitute for the wild type when coproduced with FtsX. Thus, when only FtsX was produced from the P_{lac} plasmid, ~40% of the filaments exhibited at least one site of FtsN localization and the frequency of FtsN bands normalized to cell length was ~1 per 35 μm. In contrast, when a mutant FtsE protein was produced together with FtsX, FtsN localization was observed in ~70% of the filaments and the spacing of FtsN bands was ~1 per 17 μm. By either metric, this is roughly a twofold improvement in FtsN localization. Nevertheless, cell length was about the same, 18 μm for FtsX versus ~15 μm for $FtsE^{mut}X$.

As a further control during the FtsN experiments, a portion of the filaments was used for immunolocalization of FtsZ, which does not depend on FtsEX (47). Although FtsZ rings were readily detected regardless of the FtsE or FtsX content of the cells, there were only about half as many FtsZ rings per unit cell length in filaments as in shorter cells from a population that was dividing (Table 4). For example, when cells carried the P_{lac}::$ftsE^{WT}X$ plasmid, they averaged 4.5 μm in length and the ring spacing was ~1 per 5 μm. In all other cases, the cells were about 15 μm long and ring spacing increased to ~1 per 10 μm. The twofold reduction in the frequency of FtsZ rings in filaments was expected because we observed something similar for FtsA and ZipA in our previous study of FtsEX (47) and because many reports have documented that depletion or inactivation of late division proteins has a modest deleterious effect on FtsZ rings (2, 12, 26, 39, 58). This observation may be relevant to our finding that GFP-FtsI and FtsN rings were spaced farther apart in filaments than in dividing cells. While this finding could be interpreted to mean that mutant FtsE proteins are not fully competent for recruitment of late division proteins, we suspect it is a secondary consequence of filamentation, as evidenced by the fact that we observe a similar change for FtsZ, which is not FtsEX dependent.

FtsX localizes without FtsE. To determine whether FtsE and FtsX could localize to the septal ring independently of each other, we transformed the *ftsEX* null mutant EC1215 with plasmids that expressed either *ftsE*–3×HA or *ftsX-gfp*. FtsX-GFP localized even in cells grown in LB0N (Fig. 7; also see Table S3 in the supplemental material). Localization was better in live cells than in fixed cells. In contrast, we saw few, if any, convincing instances of localization of FtsE-3×HA in cells that lacked FtsX (see Table S3 in the supplemental material), in agreement with a recent report that GFP-FtsE and FLAG-FtsE require FtsX for localization (15).

FtsX has only four TM segments. If FtsEX serves as a transporter, then the transmembrane (TM) segments in FtsX would be expected to form a substrate channel. We predicted the topology of FtsX with four publicly available computer

TABLE 4. Effect of FtsE lesions on septal localization of FtsI, FtsN, and FtsZ[a]

Assay and protein produced	Sugar or presence of NaCl	No. of cells	Length[b] (μm)	No. of rings	% Cells with ring(s)	Ring spacing[c] (μm)
Localization of GFP-FtsI						
FtsEX	Ara	187	8.1 (2.3)	186	86	8.1
	Glu	208	8.5 (3.1)	165	74	11
(−)	Ara	195	7.9 (2.3)	190	91	8.1
	Glu	169	29.7 (11.8)	124	45	40
FtsE	Ara	161	8.1 (2.5)	167	90	7.8
	Glu	107	33.7 (10.9)	81	35	45
FtsX	Ara	163	7.8 (2.2)	141	77	9.0
	Glu	108	30.0 (8.1)	67	39	48
FtsE(K41Q)X	Ara	192	8.6 (2.1)	194	89	8.5
	Glu	160	26.0 (12.2)	266	83	16
FtsE(D162A)X	Ara	169	9.8 (2.7)	173	83	9.6
	Glu	278	25.3 (12.5)	493	85	14
FtsE(E163A)X	Ara	120	10.4 (3.3)	144	86	8.7
	Glu	266	28.3 (11.7)	468	79	16
Immunofluorescence of FtsN						
FtsEX	+	181	3.3 (0.8)	78	43	7.7
	−	168	4.4 (1.1)	86	51	8.6
(−)	+	103	7.4 (4.6)	72	56	11
	−	110	17.5 (13)	55	34	35
FtsE	+	128	8.6 (4.5)	95	59	12
	−	117	15.4 (9.7)	56	35	32
FtsX	+	135	8.8 (3.7)	105	69	11
	−	130	18.2 (11.5)	67	42	35
FtsE(K41Q)X	+	135	6.5 (3.5)	86	61	10
	−	135	15.1 (8.1)	113	72	18
FtsE(D162A)X	+	74	14.4 (8.9)	79	70	13
	−	130	14.6 (6.9)	126	73	15
FtsE(E163A)X	+	125	7.5 (6.4)	72	53	13
	−	107	16.1 (11.8)	92	62	19
Immunofluorescence of FtsZ						
FtsEX	+	130	3.1 (0.9)	110	85	3.7
	−	108	4.5 (1.3)	100	93	4.9
(−)	+	135	8.6 (4.7)	168	90	6.9
	−	109	15.9 (9.4)	176	87	9.8
FtsE	+	118	8.2 (3.9)	168	92	5.8
	−	102	16.6 (11)	138	71	12
FtsX	+	123	8.3 (4)	163	89	6.3
	−	116	16.8 (9.3)	174	81	11
FtsE(K41Q)X	+	126	6.6 (2.2)	115	87	7.2
	−	99	13.5 (8.9)	130	82	10
FtsE(D162A)X	+	67	15.0 (8.8)	81	85	12
	−	119	14.4 (8.3)	175	85	9.8
FtsE(E163A)X	+	131	6.7 (2.8)	133	89	6.6
	−	119	14.9 (9.5)	167	82	11

[a] Strains used are listed in legend to Fig. 6. (−), empty vector.
[b] Mean (standard deviation).
[c] (Number of cells × length)/number of rings.

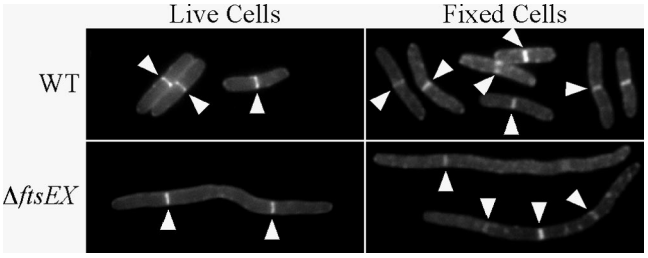

FIG. 7. FtsX-GFP localizes in cells that lack FtsE. Fluorescence microscopy was used to image FtsX-GFP in live and fixed cells of EC251 (wild type) or EC1215 (Δ*ftsEX*) harboring pDSW513 (P_{204}::*ftsX-gfp*). Arrows indicate sites of FtsX-GFP localization.

algorithms using default parameters. All four programs predicted FtsX to contain four TM segments, with the N terminus and C terminus in the cytoplasm and a large periplasmic loop (~160 amino acids) between TM1 and TM2 (Fig. 8A). To determine the number and location of all TM segments experimentally, we constructed a set of eleven *ftsX′-′phoA* fusions, using the predicted structure as a guide. The alkaline phosphatase activity of each fusion was measured and compared to that of a positive control *ftsI′-′phoA* fusion known to place the PhoA moiety in the periplasm (9). Three independent experiments showed the reporter strain harboring the *ftsI′-′phoA* fusion had an alkaline phosphatase activity of approximately 125 Miller units. Six of the eleven *ftsX′-′phoA* fusions (listed as

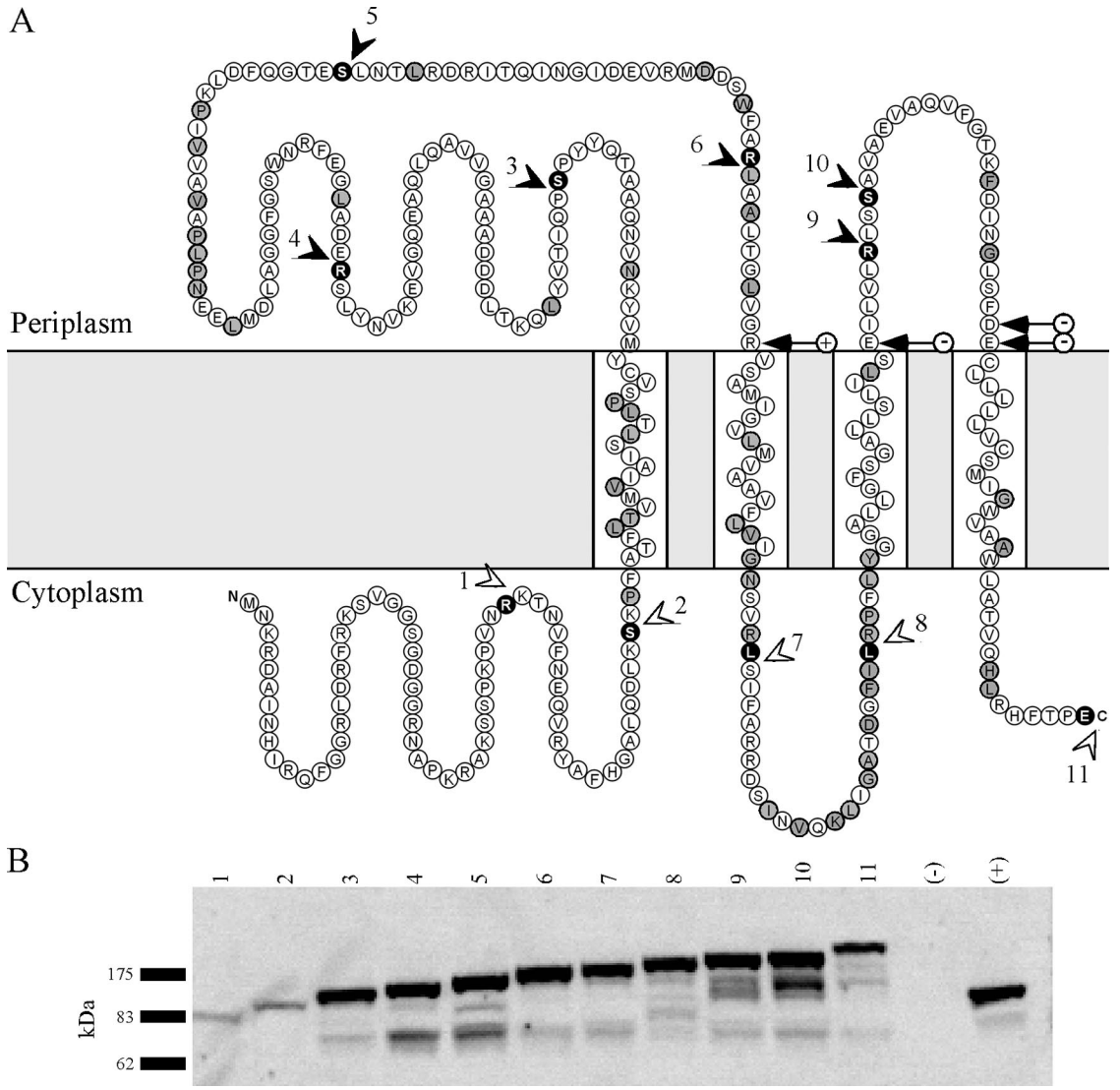

FIG. 8. Topology of FtsX. (A) Model of FtsX. Arrowheads and black residues indicate junction points of FtsX′-′PhoA fusions. Arrowheads are colored based on their activity as either high (>125 units; black) or low (<12 units; white). Arrows with circled "+" or "−" symbols indicate charged residues predicted by some computer topology programs to be within the membrane. Shaded residues are highly conserved (≥80% identity) in an alignment of FtsX proteins from *E. coli*, *Photorhabdus luminescens*, *Xylella fastidiosia*, *V. cholerae*, *H. influenzae*, *P. aeruginosa*, *Shewanella oneidensis*, *Photobacterium profundum*, *P. multocida*, *Xanthomonas axonopodis*, and *Neisseria meningitidis*. (B) Western blot of FtsX′-′PhoA fusions. Lane numbers correspond to the fusions in panel A. "(−)" is a strain with the *′phoA* fusion vector, which lacks a translational start site. "(+)" is an *ftsI′-′phoA* fusion. Molecular mass markers are indicated to the left of the blot.

3, 4, 5, 6, 9, and 10 in Fig. 8A) displayed alkaline phosphatase activity higher than that of the positive control (166 to 195 Miller units). In contrast, the other five *ftsX′-′phoA* fusions and the empty vector control exhibited <12 Miller units of activity. The results were fully consistent with the predicted topology.

Western blotting with anti-PhoA antibody confirmed that most of the fusions were expressed at comparable levels (Fig. 8B). The only exceptions were the two earliest fusions, both of which were poorly expressed and had very little PhoA activity. Thus, the low PhoA activities of these two fusions cannot be used to infer topology. Nevertheless, the N terminus of FtsX can be reliably localized to the cytoplasm, because we demonstrated previously that a GFP-FtsX fusion supports division and is fluorescent (47). GFP exported to the periplasm by the Sec system does not fold properly and fails to fluoresce (23).

To our knowledge, the TMs of most transporters contain charged amino acids that interact with charges on the substrate(s). Our model for FtsX does not show any charged residues in the membrane, but four charged residues (R223, E292, D321, and E322) are shown adjacent to the lipid bilayer on the periplasmic side, and some predictions placed some of these residues in the membrane. None of these residues is invariant among FtsX proteins from different bacterial species (Fig. 8A), making it unlikely that they play a critical role in substrate transport. To verify this inference, each charged residue was changed to alanine by site-directed mutagenesis. All

four alanine substitution derivatives complemented as well as the wild type (data not shown). It is unlikely that any of these residues is in the membrane, but even if they are, none is important for FtsEX function.

DISCUSSION

Our previous work demonstrated that FtsEX is a component of the septal ring and improves septal ring assembly, especially in media of low osmotic strength, such as LB0N (47). In particular, we showed that when cells are depleted of FtsEX, the "early" proteins in the dependency hierarchy for septal ring assembly, such as FtsZ, FtsA, and ZipA, still localize well. In contrast, the "late" proteins localize very poorly. That study left open a number of important questions, including whether FtsEX is a transporter, the mechanism(s) by which FtsEX improves septal ring assembly, and the specific contributions of FtsE and FtsX to this process. Several of the findings reported here have implications for those questions.

Evidence that FtsE uses ATP to promote septal ring constriction. We constructed and characterized three mutant FtsE proteins with lesions in the predicted ATP-binding site. These lesions had little or no effect on the ability of FtsE to localize to septal rings and recruit FtsI and FtsN. Because these are the last two (known) essential proteins in the recruitment hierarchy (3, 58), we infer that sepal rings assembled with FtsE ATP-binding site mutant proteins contain a full complement of essential division proteins. Nevertheless, the mutant *ftsE* alleles did not effectively rescue division, and filamentous cells with multiple septal rings were readily observed. Taken together, these findings imply FtsE has to handle ATP to support cell division. More intriguing, the ATP requirement appears to be for septal ring constriction rather than septal ring assembly. At the very least, ATP appears to be more important for constriction than assembly. Consistent with this interpretation, we also found one of the mutant FtsE proteins, FtsE(D162A), is a mild dominant negative that impaired division by interfering with septal ring constriction rather than septal ring assembly.

In a previous article, we suggested that FtsX might serve as a membrane anchor while FtsE uses ATP hydrolysis to improve constriction of the septal ring (47). In the meantime, Corbin and coworkers have shown that FtsE interacts directly with FtsZ (15), a tubulin-like protein that uses energy from GTP hydrolysis to drive cytokinesis (41). While evidence that FtsEX facilitates septal ring constriction dovetails nicely with the FtsE-FtsZ interaction, it is important to note that neither we (this study) nor Margolin's group have been able to show that FtsE localizes to division sites in the absence of FtsX, despite some effort. This is puzzling, because the FtsE-FtsZ interaction was strong (it stood up to coprecipitation) and independent of FtsX (15).

Two caveats concerning our inference that ATP is needed for constriction rather than assembly of the septal ring deserve mention. First, we have not investigated whether the mutant FtsE proteins support recruitment of several nonessential proteins to the septal ring (6, 7, 25, 32, 50). Although failure to recruit any one of these proteins would not account for the division defects reported here, failure to recruit several of them might. Second, we were unable to assay the ability of FtsE and its mutant derivatives to bind or hydrolyze ATP. Contrary to a previous report (20), in our hands His_6-tagged FtsE proteins were insoluble, and even the wild type failed to bind ATP reproducibly in the presence (or absence) of urea and other solubilization reagents. Thus, the mutant proteins studied here might retain some residual ability to bind and hydrolyze ATP.

Implications for the role of FtsEX in septal ring assembly. We found that depletion of FtsEX to the point that cells could no longer divide had no noticeable effect on the amounts of the late proteins FtsK, FtsQ, FtsI, or FtsN in the membrane fraction. This result all but rules out the hypothesis that FtsEX serves as a specialized ABC transporter that helps to insert some of the late Fts proteins into the cytoplasmic membrane. We favor the hypothesis that FtsEX improves septal ring assembly by engaging in protein-protein interactions. Three interactions involving FtsEX have been reported: FtsX-FtsA, FtsX-FtsQ, and FtsE-FtsZ (15, 31). Here we showed that FtsX localized reasonably well in the absence of FtsE, but localization of FtsE was not observed unless FtsX was also present. Together, these findings imply that FtsX plays a more important role than FtsE in targeting FtsEX to the septal ring, and they underscore the potential significance of the FtsX-FtsA interaction (31). We also showed that both FtsE and FtsX had to be present to facilitate recruitment of FtsI or FtsN to septal rings. This implies an FtsEX complex is needed for recruitment of late proteins despite the fact that FtsX localizes in the absence of FtsE and may bind to FtsQ (31). The FtsE requirement could mean that FtsE interacts with late proteins directly, but using bacterial two-hybrid systems, we have yet to find any interactions involving FtsE other than those expected of an ABC transporter, namely, FtsE-FtsE and FtsE-FtsX (S. J. R. Arends and D. S. Weiss, unpublished). Alternatively, FtsE might improve the ability of FtsX to interact with late proteins by improving dimerization of FtsX or modulating the conformation of FtsX's periplasmic domain. Finally, we note that the relatively long time lag that separates FtsZ ring formation from recruitment of the late proteins (1) suggests that recruitment of the late proteins is triggered by something the FtsZ ring does, in which case FtsEX could improve septal ring assembly by stimulating FtsZ ring function rather than interacting with late division proteins directly.

Membrane topology of FtsX. Any substrate that FtsEX moves across the cytoplasmic membrane would presumably pass through a channel formed by a dimer of FtsX. Here we showed that FtsX has only four TM segments, which would provide for a total of eight TM segments in an $FtsE_2X_2$ complex. Other noteworthy features of the topology are the absence of charged amino acids in the TM segments and the presence of a large periplasmic loop between TM1 and TM2. An independent study arrived at a similar topology model for FtsX based on a combination of computer predictions, one GFP fusion and one PhoA fusion (17). The structure of FtsX seems most compatible with a substrate that is small and uncharged. But in our view, the structure of FtsX is not very suggestive of a transporter at all, and we wonder whether FtsE uses ATP hydrolysis to drive an event in the periplasm, where FtsX has a conspicuously large domain. If so, the TM segments of FtsX would transmit a conformation change rather than forming a substrate channel.

Support for this hypothesis comes from consideration of the two ABC transporters most closely related to FtsEX. These are MacB and LolCDE, both of which have only four TM segments per integral membrane domain and assemble into ABC transporters with a total of eight TM segments (8, 17, 34). LolC and LolD work together with the cytoplasmic ATPase LolE to transfer lipoproteins from the outer surface of the cytoplasmic membrane to the periplasmic chaperone LolA (52, 60). This activity does not involve moving a substrate across a membrane, and the TM segments of LolC and LolD serve to transmit ATP-driven conformation changes rather than forming a substrate channel. The role of the TM segments in MacB is less clear. On one hand, MacB helps to secrete heat-stable enterotoxin II from the periplasm across the outer membrane (61). Enterotoxin II crosses the outer membrane via TolC rather than MacB, so the TM segments of MacB do not function as a substrate channel in this process. On the other hand, MacB also affords weak protection against macrolide antibiotics. These drugs might cross the cytoplasmic membrane via a channel in MacB, but there are unresolved discrepancies among the various studies, and the actual role of MacB in this process is obscure (35, 37, 51).

ACKNOWLEDGMENTS

We thank Joe Lutkenhaus for anti-FtsK, Andrew Hawkins for a *phoA* vector, L. Paolozzi, G. Karimova, and D. Ladant for bacterial two-hybrid plasmids and strains, Bruce Ayati for the formula used to calculate division events for mutants in LB0N, and Kari Schmidt and Jennifer Wendt for constructing some of the strains and plasmids used in this study. We are grateful to members of the Weiss laboratory for helpful discussions.

This work was supported in part by a grant from the National Institutes of Health (GM59893) to D.S.W. and by funds from the Department of Microbiology. S.J.R.A. was supported by an NIH Training Grant in Biotechnology (T32 GM08365-13). The DNA Facility is supported through the Holden Comprehensive Cancer Center's Cancer Center Support Grant 2 P30 CA086862 from the National Cancer Institute/NIH and the Carver College of Medicine, University of Iowa.

REFERENCES

1. **Aarsman, M. E., A. Piette, C. Fraipont, T. M. Vinkenvleugel, M. Nguyen-Disteche, and T. den Blaauwen.** 2005. Maturation of the *Escherichia coli* divisome occurs in two steps. Mol. Microbiol. **55:**1631–1645.
2. **Addinall, S. G., E. Bi, and J. Lutkenhaus.** 1996. FtsZ ring formation in *fts* mutants. J. Bacteriol. **178:**3877–3884.
3. **Addinall, S. G., C. Cao, and J. Lutkenhaus.** 1997. FtsN, a late recruit to the septum in *Escherichia coli*. Mol. Microbiol. **25:**303–309.
4. **Arends, S. J. R., K. B. Williams, R. J. Kustusch, and D. S. Weiss.** 2007. Cell division, p. 173–197. *In* M. Ehrmann (ed.), The periplasm. ASM Press, Washington, DC.
5. **Ausubel, F. A., R. Brent, R. E. Kingston, D. D. Moore, J. G. Seidman, J. A. Smith, and K. Struhl.** 1998. Current protocols in molecular biology. John Wiley & Sons, New York, NY.
6. **Bernhardt, T. G., and P. A. de Boer.** 2003. The *Escherichia coli* amidase AmiC is a periplasmic septal ring component exported via the twin-arginine transport pathway. Mol. Microbiol. **48:**1171–1182.
7. **Bernhardt, T. G., and P. A. de Boer.** 2004. Screening for synthetic lethal mutants in *Escherichia coli* and identification of EnvC (YibP) as a periplasmic septal ring factor with murein hydrolase activity. Mol. Microbiol. **52:** 1255–1269.
8. **Bouige, P., D. Laurent, L. Piloyan, and E. Dassa.** 2002. Phylogenetic and functional classification of ATP-binding cassette (ABC) systems. Curr. Protein Pept. Sci. **3:**541–559.
9. **Bowler, L. D., and B. G. Spratt.** 1989. Membrane topology of penicillin-binding protein 3 of *Escherichia coli*. Mol. Microbiol. **3:**1277–1286.
10. **Boyd, D., D. S. Weiss, J. C. Chen, and J. Beckwith.** 2000. Towards single-copy gene expression systems making gene cloning physiologically relevant: lambda InCh, a simple *Escherichia coli* plasmid-chromosome shuttle system. J. Bacteriol. **182:**842–847.
11. **Carson, M. J., J. Barondess, and J. Beckwith.** 1991. The FtsQ protein of *Escherichia coli*: membrane topology, abundance, and cell division phenotypes due to overproduction and insertion mutations. J. Bacteriol. **173:**2187–2195.
12. **Chen, J. C., D. S. Weiss, J. M. Ghigo, and J. Beckwith.** 1999. Septal localization of FtsQ, an essential cell division protein in *Escherichia coli*. J. Bacteriol. **181:**521–530.
13. **Cherepanov, P. P., and W. Wackernagel.** 1995. Gene disruption in *Escherichia coli*: TcR and KmR cassettes with the option of Flp-catalyzed excision of the antibiotic-resistance determinant. Gene **158:**9–14.
14. **Claros, M. G., and G. von Heijne.** 1994. TopPred II: an improved software for membrane protein structure predictions. Comput. Appl. Biosci. **10:**685–686.
15. **Corbin, B. D., Y. Wang, T. K. Beuria, and W. Margolin.** 2007. Interaction between cell division proteins FtsE and FtsZ. J. Bacteriol. **189:**3026–3035.
16. **Dai, K., Y. Xu, and J. Lutkenhaus.** 1996. Topological characterization of the essential *Escherichia coli* cell division protein FtsN. J. Bacteriol. **178:**1328–1334.
17. **Daley, D. O., M. Rapp, E. Granseth, K. Melen, D. Drew, and G. von Heijne.** 2005. Global topology analysis of the *Escherichia coli* inner membrane proteome. Science **308:**1321–1323.
18. **Datsenko, K. A., and B. L. Wanner.** 2000. One-step inactivation of chromosomal genes in *Escherichia coli* K-12 using PCR products. Proc. Natl. Acad. Sci. USA **97:**6640–6645.
19. **Davidson, A. L., E. Dassa, C. Orelle, and J. Chen.** 2008. Structure, function, and evolution of bacterial ATP-binding cassette systems. Microbiol. Mol. Biol. Rev. **72:**317–364.
20. **de Leeuw, E., B. Graham, G. J. Phillips, C. M. ten Hagen-Jongman, B. Oudega, and J. Luirink.** 1999. Molecular characterization of *Escherichia coli* FtsE and FtsX. Mol. Microbiol. **31:**983–993.
21. **Dorazi, R., and S. J. Dewar.** 2000. Membrane topology of the N-terminus of the *Escherichia coli* FtsK division protein. FEBS Lett. **478:**13–18.
22. **Erickson, J. W., V. Vaughn, W. A. Walter, F. C. Neidhardt, and C. A. Gross.** 1987. Regulation of the promoters and transcripts of *rpoH*, the *Escherichia coli* heat shock regulatory gene. Genes Dev. **1:**419–432.
23. **Feilmeier, B. J., G. Iseminger, D. Schroeder, H. Webber, and G. J. Phillips.** 2000. Green fluorescent protein functions as a reporter for protein localization in *Escherichia coli*. J. Bacteriol. **182:**4068–4076.
24. **Garti-Levi, S., R. Hazan, J. Kain, M. Fujita, and S. Ben-Yehuda.** 2008. The FtsEX ABC transporter directs cellular differentiation in *Bacillus subtilis*. Mol. Microbiol. **69:**1018–1028.
25. **Gerding, M. A., Y. Ogata, N. D. Pecora, H. Niki, and P. A. de Boer.** 2007. The trans-envelope Tol-Pal complex is part of the cell division machinery and required for proper outer-membrane invagination during cell constriction in *E. coli*. Mol. Microbiol. **63:**1008–1025.
26. **Ghigo, J. M., D. S. Weiss, J. C. Chen, J. C. Yarrow, and J. Beckwith.** 1999. Localization of FtsL to the *Escherichia coli* septal ring. Mol. Microbiol. **31:**725–737.
27. **Goehring, N. W., and J. Beckwith.** 2005. Diverse paths to midcell: assembly of the bacterial cell division machinery. Curr. Biol. **15:**R514–R526.
28. **Guzman, L. M., D. Belin, M. J. Carson, and J. Beckwith.** 1995. Tight regulation, modulation, and high-level expression by vectors containing the arabinose P_{BAD} promoter. J. Bacteriol. **177:**4121–4130.
29. **Haldimann, A., and B. L. Wanner.** 2001. Conditional-replication, integration, excision, and retrieval plasmid-host systems for gene structure-function studies of bacteria. J. Bacteriol. **183:**6384–6393.
30. **Hashimoto-Gotoh, T., M. Yamaguchi, K. Yasojima, A. Tsujimura, Y. Wakabayashi, and Y. Watanabe.** 2000. A set of temperature sensitive-replication/-segregation and temperature resistant plasmid vectors with different copy numbers and in an isogenic background. Gene **241:**185–191.
31. **Karimova, G., N. Dautin, and D. Ladant.** 2005. Interaction network among *Escherichia coli* membrane proteins involved in cell division as revealed by bacterial two-hybrid analysis. J. Bacteriol. **187:**2233–2243.
32. **Karimova, G., C. Robichon, and D. Ladant.** 2009. Characterization of YmgF, a 72-residue inner membrane protein that associates with the *Escherichia coli* cell division machinery. J. Bacteriol. **191:**333–346.
33. **Kempf, M. J., and M. J. McBride.** 2000. Transposon insertions in the *Flavobacterium johnsoniae ftsX* gene disrupt gliding motility and cell division. J. Bacteriol. **182:**1671–1679.
34. **Kobayashi, N., K. Nishino, T. Hirata, and A. Yamaguchi.** 2003. Membrane topology of ABC-type macrolide antibiotic exporter MacB in *Escherichia coli*. FEBS Lett. **546:**241–246.
35. **Kobayashi, N., K. Nishino, and A. Yamaguchi.** 2001. Novel macrolide-specific ABC-type efflux transporter in *Escherichia coli*. J. Bacteriol. **183:**5639–5644.
36. **Krogh, A., B. Larsson, G. von Heijne, and E. L. Sonnhammer.** 2001. Predicting transmembrane protein topology with a hidden Markov model: application to complete genomes. J. Mol. Biol. **305:**567–580.
37. **Lin, H. T., V. N. Bavro, N. P. Barrera, H. M. Frankish, S. Velamakanni, H. W. van Veen, C. V. Robinson, M. I. Borges-Walmsley, and A. R. Walmsley.** 2009. MacB ABC transporter is a dimer whose ATPase activity and macrolide-

binding capacity are regulated by the membrane fusion protein MacA. J. Biol. Chem. **284:**1145–1154.
38. **Manoil, C.** 1991. Analysis of membrane protein topology using alkaline phosphatase and beta-galactosidase gene fusions. Methods Cell Biol. **34:**61–75.
39. **Mercer, K. L., and D. S. Weiss.** 2002. The *Escherichia coli* cell division protein FtsW is required to recruit its cognate transpeptidase, FtsI (PBP3), to the division site. J. Bacteriol. **184:**904–912.
40. **Merino, S., M. Altarriba, R. Gavin, L. Izquierdo, and J. M. Tomas.** 2001. The cell division genes (*ftsE* and *X*) of *Aeromonas hydrophila* and their relationship with opsonophagocytosis. FEMS Microbiol. Lett. **198:**183–188.
41. **Osawa, M., D. E. Anderson, and H. P. Erickson.** 2008. Reconstitution of contractile FtsZ rings in liposomes. Science **320:**792–794.
42. **Pogliano, J., K. Pogliano, D. S. Weiss, R. Losick, and J. Beckwith.** 1997. Inactivation of FtsI inhibits constriction of the FtsZ cytokinetic ring and delays the assembly of FtsZ rings at potential division sites. Proc. Natl. Acad. Sci. USA **94:**559–564.
43. **Ramirez-Arcos, S., H. Salimnia, I. Bergevin, M. Paradis, and J. A. Dillon.** 2001. Expression of *Neisseria gonorrhoeae* cell division genes *ftsZ*, *ftsE* and *minD* is influenced by environmental conditions. Res. Microbiol. **152:**781–791.
44. **Reddy, M.** 2007. Role of FtsEX in cell division of *Escherichia coli*: viability of *ftsEX* mutants is dependent on functional SufI or high osmotic strength. J. Bacteriol. **189:**98–108.
45. **Salmond, G. P., and S. Plakidou.** 1984. Genetic analysis of essential genes in the *ftsE* region of the *Escherichia coli* genetic map and identification of a new cell division gene, *ftsS*. Mol. Gen. Genet. **197:**304–308.
46. **Sarkar, G., and S. S. Sommer.** 1990. The "megaprimer" method of site-directed mutagenesis. BioTechniques **8:**404–407.
47. **Schmidt, K. L., N. D. Peterson, R. J. Kustusch, M. C. Wissel, B. Graham, G. J. Phillips, and D. S. Weiss.** 2004. A predicted ABC transporter, FtsEX, is needed for cell division in *Escherichia coli*. J. Bacteriol. **186:**785–793.
48. **Strauch, K. L., and J. Beckwith.** 1988. An *Escherichia coli* mutation preventing degradation of abnormal periplasmic proteins. Proc. Natl. Acad. Sci. USA **85:**1576–1580.
49. **Sun, Q., X. C. Yu, and W. Margolin.** 1998. Assembly of the FtsZ ring at the central division site in the absence of the chromosome. Mol. Microbiol. **29:**491–503.
50. **Tarry, M., S. J. R. Arends, P. Roversi, E. Piette, F. Sargent, B. C. Berks, D. S. Weiss, and S. M. Lea.** 2009. The *Escherichia coli* cell division protein and model Tat substrate SufI (FtsP) localizes to the septal ring and has a multicopper oxidase-like structure. J. Mol. Biol. **386:**504–519.
51. **Tikhonova, E. B., V. K. Devroy, S. Y. Lau, and H. I. Zgurskaya.** 2007. Reconstitution of the *Escherichia coli* macrolide transporter: the periplasmic membrane fusion protein MacA stimulates the ATPase activity of MacB. Mol. Microbiol. **63:**895–910.
52. **Tokuda, H., and S. Matsuyama.** 2004. Sorting of lipoproteins to the outer membrane in *E. coli*. Biochim. Biophys. Acta **1693:**5–13.
53. **Tusnady, G. E., and I. Simon.** 2001. The HMMTOP transmembrane topology prediction server. Bioinformatics **17:**849–850.
54. **Ukai, H., H. Matsuzawa, K. Ito, M. Yamada, and A. Nishimura.** 1998. *ftsE*(Ts) affects translocation of K^+-pump proteins into the cytoplasmic membrane of *Escherichia coli*. J. Bacteriol. **180:**3663–3670.
55. **Vicente, M., A. I. Rico, R. Martinez-Arteaga, and J. Mingorance.** 2006. Septum enlightenment: assembly of bacterial division proteins. J. Bacteriol. **188:**19–27.
56. **Wang, L., and J. Lutkenhaus.** 1998. FtsK is an essential cell division protein that is localized to the septum and induced as part of the SOS response. Mol. Microbiol. **29:**731–740.
57. **Weiss, D. S.** 2004. Bacterial cell division and the septal ring. Mol. Microbiol. **54:**588–597.
58. **Weiss, D. S., J. C. Chen, J. M. Ghigo, D. Boyd, and J. Beckwith.** 1999. Localization of FtsI (PBP3) to the septal ring requires its membrane anchor, the Z ring, FtsA, FtsQ, and FtsL. J. Bacteriol. **181:**508–520.
59. **Wissel, M. C., and D. S. Weiss.** 2004. Genetic analysis of the cell division protein FtsI (PBP3): amino acid substitutions that impair septal localization of FtsI and recruitment of FtsN. J. Bacteriol. **186:**490–502.
60. **Yakushi, T., K. Masuda, S. Narita, S. Matsuyama, and H. Tokuda.** 2000. A new ABC transporter mediating the detachment of lipid-modified proteins from membranes. Nat. Cell Biol. **2:**212–218.
61. **Yamanaka, H., H. Kobayashi, E. Takahashi, and K. Okamoto.** 2008. MacAB is involved in the secretion of *Escherichia coli* heat-stable enterotoxin II. J. Bacteriol. **190:**7693–7698.